Available online at www.sciencedirect.com

ScienceDirect

journal homepage: www.intl.elsevierhealth.com/journals/dema

Evaluation of the filler packing structures in dental resin composites: From theory to practice

Ruili Wang[a,b], *Eric Habib*[a], *X.X. Zhu*[a,*]

[a] *Département de Chimie, Université de Montréal, C.P. 6128, Succursale Centre-ville, Montreal, QC, H3C 3J7, Canada*
[b] *State Key Laboratory for Modification of Chemical Fibers and Polymer Materials, College of Material Science and Engineering, Donghua University, Shanghai 201620, China*

ARTICLE INFO

Article history:
Received 15 February 2018
Accepted 24 March 2018

Keywords:
Spherical particles
Close-packed structures
Random-packed structures
Dental composites
Mechanical properties
Polymerization shrinkage
Rheology

ABSTRACT

Objectives. The aim of this study is to evaluate the packing properties of uniform silica particles and their mixture with secondary particles yielding maximally loaded dental composites. We intend to verify the difference between the idealized models (the close-packed structures and the random-packed structures) and the actual experimental results, in order to provide guidance for the preparation of dental composites. The influence of secondary particle size and the resin composition on the physical–mechanical properties and the rheological properties of the experimental dental composites was also investigated.

Methods. Silica particles (S-920, S-360, and S-195) with average diameters of 920, 360, and 195 nm were synthesized via the Stöber process. Their morphology and size distribution were determined by field-emission scanning electron microscopy and laser particle sizer. A series of silica fillers, S-920, S-920+195, S-920+360, and S-920+360+195, were then formulated with two Bis-GMA/TEGDMA resins (weight ratios of 70:30 and 50:50). For these experimental dental composites, their maximum filler loadings were assessed and compared to the theory. The mechanical properties, degree of conversion, depth of cure, and polymerization shrinkage of these composites were then evaluated. Their rheological behaviors were measured with a rheometer.

Results. Unimodal S-920 had the maximally filler loading of 70.80 wt% with the 5B5T resin, close to the theoretical estimation of the random loose packing (71.92 wt%). The maximum loading of the S-920+360+195 filled composite was 72.92 wt% for the same resin, compared to the theoretical estimation of 89.29 wt% obtained for the close-packed structures. These findings indicate that random loose packing matches more closely to the real packing state for the filler formulations used. When maximally loaded, the composite with S-920+360+195 produced the best mechanical properties and the lowest polymerization shrinkage. The degree of conversion and depth of cure were higher with secondary particles added, and the viscosity of all unpolymerized pastes exhibited shear thinning behavior.

Significance. Theoretical estimations of filler packing structures provide a useful guidance in the design of multimodal filler formulations and the preparation of dental composites with higher filler loading, improved physical–mechanical properties.

* *Corresponding author.*
E-mail address: julian.zhu@umontreal.ca (X.X. Zhu).
https://doi.org/10.1016/j.dental.2018.03.022

1. Introduction

Light-curable dental resin composites are now widely used as filling materials for repairing damaged or decayed tooth structure, mainly due to their superior esthetic appearance [1]. These composites primarily consist of a polymerizable resin matrix and the silanized inorganic fillers [2]. The most commonly seen morphologies of inorganic fillers are spherical or irregular [3]. Apart from the work on different commercial composites, some studies also examined the influence of filler morphology on properties of dental composites. Satterthwaite et al. found that the composites with spherical fillers had lower values of shrinkage stress and strain in comparison to irregular fillers [4,5]. For the composites with multimodal spherical fillers, the incorporation of smaller particles also improved the shrinkage-strain as well as the wear performance [6]. Although the use of hybrid fillers has been reported, the choice of the multimodal filler formulations is often based on empirical estimates. A more rational formulation with theoretical guidance is needed to minimize the amount of work needed and also to improve the performance of the final composites. For practical reasons, spherical particles are used in this work, as they often showed lower shrinkage-stress and shrinkage-strain, reducing the occurrence of secondary caries in clinical applications [4,5]. Additionally, they are also much easier to model.

We examined the theory of close-packed structures of identical spherical particles, including face centered cubic (FCC) and hexagonal close packed (HCP), in dental composites [7]. The highest packing factor (74.05 vol%) of this theoretical model indicates that identical spheres cannot completely fill the entire space [8,9]; thus for dental composites, the remaining voids can be occupied with the resin matrix and secondary particles. The maximum size of secondary spherical particles which can fit into a tetrahedral void ($d_4 = 0.225\ D$) and an octahedral void ($d_8 = 0.414\ D$) of primary particles is also studied, where D is the diameter of the close-packed primary spheres, and d_4 and d_8 are the diameters of the particles that may fit xactly into the tetrahedral and octahedral voids, respectively. For a representative primary spherical particle (D = 1000 nm), the best packing factor is increased to 81.19 vol% after embedding two secondary particles with the respective sizes of 225 nm (d_4) and 414 nm (d_8) into the tetrahedral voids and octahedral voids of primary particles. This packing factor is higher than the structure embedded by either one of these secondary particles. Such theoretical calculations may not be the exact situation for the dental composites due to the viscosity of the materials upon the addition of monomers, but it would be interesting to test it and use as a guideline in the optimization of the multimodal filler formulations for dental resin composites.

After being loaded with fillers, the viscosity of uncured composite pastes determines the way materials flow and thus their handling properties for dentists. Much effort was made to study the effects of the composition and ratio of resin monomers and the filler composition, including filler loading, morphology, and size distribution [10–13]. However, no previous work has explored the rheological properties of dental composites with spherical particles at the highest loading levels.

The objective of this study is to evaluate the use of all the theoretical estimations in the formulation of dental composites of two different compositions of dental monomers (7B3T and 5B5T) designed to affect the viscosity of the pastes. The effects of the secondary particle size and the viscosity of two resins on the maximum filler loading, the physical–mechanical properties, and the rheological behavior of dental composites have also studied to point out the accordance and deviation of the theoretical model in the practical formulation of dental composites.

2. Materials and methods

2.1. Materials

Tetraethoxysilane (TEOS) was purchased from Alfa Aesar (Haverhill, MA, USA). Ammonium hydroxide (35 wt%) and anhydrous ethanol were purchased from Fisher Scientific (Waltham, MA, USA). 3-methacryloyltrimethoxypropylsilane (γ-MPS), bisphenol A glycerolate dimethacrylate (Bis-GMA), and triethylene glycol dimethacrylate (TEGDMA) were purchased from VWR (Radnor, PA, USA). Camphorquinone (CQ) and ethyl 4-dimethylamino benzoate (4-EDMAB) were purchased from Sigma-Aldrich (Oakville, ON, Canada). All chemicals were used without further purification.

2.2. Methods

2.2.1. Synthesis of monodisperse silica particles and characterization

Monodisperse silica particles (S-920, S-360, and S-195) with the respective average diameters of 920, 360, and 195 nm were synthesized using the Stöber method [14], as described in our previous work [3,15]. All these particles obtained were silanized with γ-MPS following a previously used method before mixing with the resin matrix [3]. Here, S-920 is used as primary particles while S-360 and S-195 serve as secondary particles, which will theoretically fit into the voids of FCC and HCP structures of the close-packed S-920.

The size of silica particles was determined with laser diffraction (Horiba Laser Particle Sizer LA-950, Japan) in water. Field-emission scanning electron microscopy (JEOL JSM-7400F FE-SEM, Japan) was further used to confirm their size, dispersity, and morphology with an accelerating voltage of 1.5 kV.

2.2.2. Preparation of dental composites

The resin matrix was first prepared by dissolving CQ and 4-EDMAB (0.5/0.5, wt/wt; total concentration: 1 wt% of the final resin) into the resin monomers (Bis-GMA/TEGDMA) under magnetic stirring at room temperature (RT, 23 °C) for 6 h. In consideration of the common compositions of resin monomers reported previously [16–18] and to vary the viscosity of the resins, the weight ratios of Bis-GMA/TEGDMA were fixed at 50:50 and 70:30 in this study, respectively, abbreviated as 5B5T and 7B3T, with the respective viscosities of 0.201 and 2.29 Pa s reported in the literature [13].

Table 1 – Compositions of inorganic fillers used in this study.

Filler type	Average filler size (nm)	Code
Unimodal silica	920	S-920
Bimodal silica	920 and 195	S-920+195
	920 and 360	S-920+360
Trimodal silica	920, 360, and 195	S-920+360+195

Dental composites were reinforced with the unimodal, bimodal, and trimodal silica fillers, as specified in Table 1. To determine their maximum loading, unimodal S-920 was first added and premixed with the liquid resin matrix by spatula, and further blended with a three-roll mixer (EXAKT 50I, Norderstedt, Germany). Once the composite was no longer cohesive and turned into discontinuous fragments, it was overloaded, and the value before the last addition served as the maximum filler loading of S-920. Secondary fillers (S-195 or/and S-360) were then maximally added to the highest loaded S-920 composite on the three-roll mixer, and the final loadings of bimodal and trimodal silica were also obtained with the method above. It should be noted that for the composite filled with S-920+360+195, S-360 was first added into the maximum loaded S-920 composite followed by S-195, and the volume ratio of S-360 to S-195 is fixed at 3.16/1 (vol/vol), based on the estimate from the theoretical FCC/HCP packing as illustrated in Table 2.

For the composites used for rheology measurements, no photo-initiators were added to make sure that the properties studied were not influenced by possible polymerization.

2.2.3. *Characterization of dental composites*

2.2.3.1. Mechanical properties. Composite bars (n = 6) were made from each composite paste using split stainless-steel bar molds of 25 mm × 2 mm × 2 mm sandwiched between two 0.5 mm thick glass slides. Cylindrical shaped composites (Φ 4 mm × 6 mm, n = 6) were prepared with the silicon rubber molds, covering the top with glass slides. All these uncured samples were polymerized with a curing lamp (Optilux 401, 400 mW/cm^2, Kerr Corporation, USA) for 20 s (3 times to cover the whole bar) and then 10 s from the other side (3 times again). The distance between the light tip and the sample surface was kept at 3–5 mm. All specimens were polished with a silicon carbide paper (P1200 grit) before testing.

Mechanical properties, including flexural strength (FS), flexural modulus (FM), and compressive strength (CS) of dental composites were then determined with a universal testing machine (Instron 33R 4201, USA). Rectangular-shaped specimens and cylindrical samples were prepared for the three-point bending tests (20 mm span, 0.75 mm/min cross-head speed) and compression tests (0.75 mm/min loading rate), respectively [19].

2.2.3.2. Degree of conversion. The conversion of dental composites was determined by Raman spectroscopy (Renishaw InVia confocal microscope, Gloucestershire, UK) under 785-nm excitation laser. The composite paste (weight: 5–10 mg; thickness: 0.5 mm) was placed on aluminum foil and measured at the top surface, then polymerized with the lamp mentioned above for 60 s and measured again. The distance between the light tip and the sample surface was also kept at 3–5 mm. Triplicate measurements were performed for each composite. Degree of conversion (Conv.) of dental composites was then determined from the ratio of absorbance intensities of aliphatic C=C bond (1638 cm^{-1}) against internal reference of aromatic C=C bond (1608 cm^{-1}) before and after curing of the specimen as shown in Eq. (1) [3,19]:

$$Conv.(\%) = \left(1 - \frac{R_{cured}}{R_{uncured}}\right) \times 100\% \quad (1)$$

where $R_{uncured}$ is band height at 1638 cm^{-1}/band height at 1608 cm^{-1} before curing, and R_{cured} is band height at 1638 cm^{-1}/band height at 1608 cm^{-1} after curing.

2.2.3.3. Depth of cure. For the depth of cure measurements, the composite paste was filled into a cylindrical mold (diameter of 4 mm, height of 10 mm), and polymerized for 20 s by shining light with the lamp on the top, according to ISO 4049-2009 [20]. The sample was then demolded, and any uncured material was removed from the bottom with a spatula. The depth of cured material was measured with a digital caliper (CD-6" CSX, Mitutoyo Corp., Japan) to an accuracy of ± 0.01 mm (n = 3).

2.2.3.4. Polymerization shrinkage. Polymerization shrinkage of dental composites was measured according to the Archimedes' principle [21]. This method determines the den-

Table 2 – Maximum volume fractions of secondary particles evaluated from the close-packed structures (FCC/HCP) to the experimental results.

Filler formulation	Maximum volume fraction of secondary silica particles					
	Theoretical estimation (FCC/HCP[a])		Experimental result			
			7B3T		5B5T	
	S-195	S-360	S-195	S-360	S-195	S-360
S-920	–	–	–	–	–	–
S-920+195	2.12	–	1.79	–	1.90	–
S-920+360	–	4.45	–	4.00	–	4.12
S-920+360+195	1.41	4.45	1.26	3.98	1.29	4.08

[a] Face centered cubic and hexagonal close packed.

sities of the unpolymerized and polymerized composites by measuring their weights in air and water, using an analytical balance (ML 204, Mettler Toledo, Switzerland) equipped with a density kit. For the measurements of unpolymerized composites, each material paste was molded into six ball-shaped specimens of mass 0.5 g using gloved fingers, avoiding the formation of air inclusions. For polymerized ones, disc specimens (diameter of 10 mm, thickness of 1 mm; n = 6) were prepared and cured for 60 s with the lamp from each side to ensure the complete conversion. Shrinkage was calculated with Eq. (2) [19]:

$$Shrinkage(\%) = \left(\frac{\rho_{cured} - \rho_{uncured}}{\rho_{cured}}\right) \times 100\% \quad (2)$$

where $\rho_{uncured}$ and ρ_{cured} are respectively the densities (g/cm^3) of the sample before and after cure.

2.2.3.5. *Fracture morphology of dental composites*. Fracture surfaces of the selected dental composites after the three-point bending tests were evaluated with FE-SEM. Each sample was gold sputter-coated before observation.

2.2.3.6. *Rheological measurement*. The rheological properties of uncured dental composites were studied by the use of a rotational rheometer (ARES, TA Instruments Co., USA) at RT. The parallel plate mode (25 mm) with a sample gap of 2 mm was adopted. The composite samples were made using the stainless-steel molds of Φ 25 mm × 2 mm between two 0.5 mm thick glass slides, and then demolded and transferred onto the parallel plate. Dynamic strain sweep tests were performed at a constant frequency of 1 Hz to determine the linear region of deformation of each sample. Dynamic frequency sweep measurements were then performed from 100 to 0.01 rad/s to determine the complex viscosity (η^*) as a function of the frequency, as described in a previous report [22].

2.3. Statistical analysis

The acquired data were statistically analyzed with one-way analysis of variance (ANOVA), followed by Tukey's test at the 95% confidence level, using SPSS software (version 13.0, Chicago, USA). Differences were considered significant at a probability of $p < 0.05$.

3. Results and discussion

3.1. Size and morphology of silica particles

The spherical silica particles exhibited average diameters of 920, 360, and 195 nm, respectively (Fig. 1). Their sizes measured from the FE-SEM images (25 random particles) and the Horiba particle sizer are listed in Fig. 1, all showing low size dispersity.

In this study, S-920 is used as the primary particles, whereas the smaller S-195 and S-360 serve as secondary particles. The size of the secondary silica fillers to be used was determined by the theoretical calculation of the maximum filler size for spherical particles in close packed tetrahedral ($d_4 = 0.225$ $D = 207$ nm) and octahedral voids ($d_8 = 0.414$ $D = 380$ nm), where D is the diameter of the primary S-920 [7,8]. Therefore, S-360 is considered to fit only into the octahedral voids, and S-195 into both tetrahedral and octahedral voids of the FCC and HCP structures, depending on the filler formulations.

3.2. Evaluation of the maximum filler loading

3.2.1. Theoretical estimations

For the fully ordered FCC and HCP models, the sliding friction between particles is neglected, and thus the packing factor of the close-packed S-920 is 74.05 vol% [7]. Secondary particles are then embedded into the voids left by the close-packed primary particles. Fig. 2 shows the theoretical void models of the representative trimodal filler S-920+360+195, based on the close-packing of S-920. In this ideal case, S-360 fit only into the octahedral voids whereas S-195 fit into the remaining tetrahedral voids.

According to the number and the volume of tetrahedral and octahedral voids in a unit cell of FCC and HCP reported in our previous work [7], the close-packed structures are then used to theoretically calculate the volume fractions of the embedded secondary particles (v_{sp}) of the filler formulations (Table 2) with Eq. (3) to further estimate their final filler loadings:

$$v_{sp}\ (vol\%) = \frac{V_{sp}}{V_c} \times 100\% \quad (3)$$

where V_{sp} is the volume of secondary particles, and V_c is the volume of a unit cell [7,23]. The detailed calculation is provided in Supporting information (Table S1).

Based on the results above (Table 2), the theoretical maximum loading of the composites filled with S-920 is first calculated as 84.98 and 85.67 wt% with 7B3T and 5B5T (Table 3), where the density of these two resins are measured to be 1.11 and 1.05 g/cm^3, respectively. The theoretical calculation of the maximum loadings of bimodal and trimodal fillers are performed with the volume fractions of secondary particles (Table 2), and the results are listed in Table 3. Details are provided in Supporting information (Calculation 2).

Furthermore, random packing is also introduced as a theoretical model, considering the sliding friction between particles. The upper and lower state of this packing is random close packing (RCP; applying to smooth spheres) and random loose packing (RLP; highly frictional spheres), with the packing factor ranging between 64 and 55 vol%, respectively [24–26]. These two packing values are also converted into the filler loadings with 7B3T and 5B5T resins (Table 3) using the method described in Supporting information (Calculation 2). As shown in Table 3, the highest theoretical loading can be achieved by the use of S-920+360+195.

3.2.2. Experimental results

Using the theoretical estimates shown in Tables 2 and 3, we prepared dental composites with two resins compositions. (1) For the unimodal composites, S-920 has a maximum loading of 70.00 and 70.80 wt% for 7B3T and 5B5T, respectively, closer to the theoretical values 70.78 and 71.92 wt% calculated from RLP, rather than 85 wt% from FCC/HCP or 78 wt% from RCP. (2) For the bimodal composites, secondary particles were further maximally added into the highest loaded

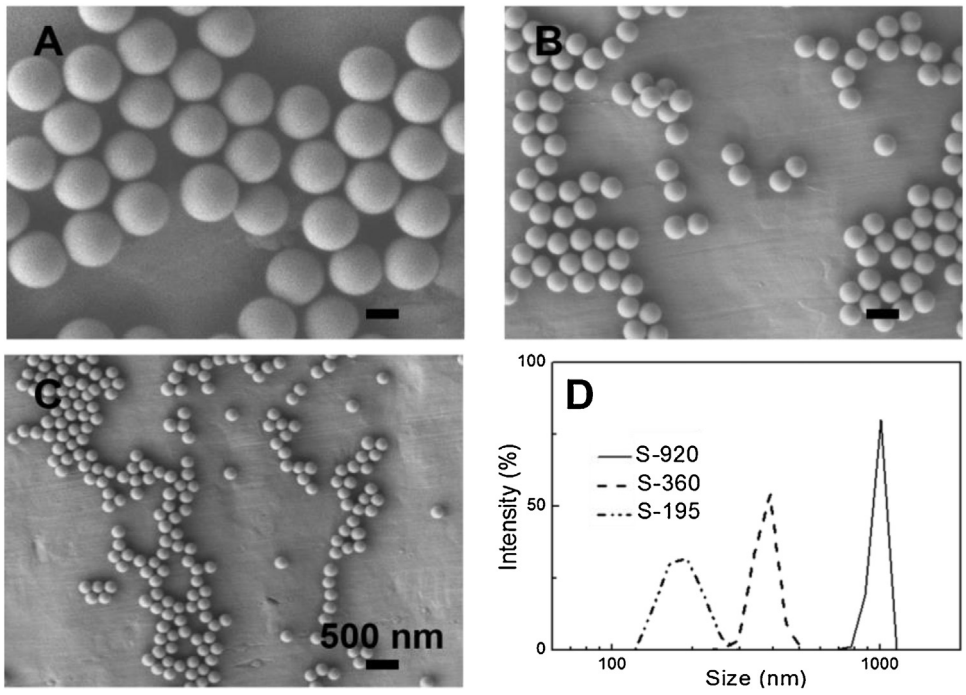

Silica particle	Average size ± SD (nm)	
	FE-SEM	Horiba particle sizer
S-920	920 ± 12	920 ± 35
S-360	360 ± 7	360 ± 23
S-195	195 ± 9	195 ± 14

Fig. 1 – FE-SEM images of S-920 (A), S-360 (B), S-195 (C), size distributions (D) and size measurements from FE-SEM images and laser light diffraction.

S-920 composites during the experiments. Both the maximum volume fractions of secondary particles and the maximum silica filler loadings (Tables 2 and 3) are obviously lower than the theoretical estimates. (3) For the trimodal composites, the mass ratio of S-360 to S-195 (3.98/1.26 = 3.16/1, vol/vol, for 7B3T and 4.08/1.29 = 3.16/1, vol/vol, for 5B5T) is found by trials, which is in accordance with the theoretical calculation (4.45/1.41 = 3.16/1, vol/vol) shown in Table 2. In comparison to the theoretical estimates, the maximum volume fractions of secondary particles and the maximum trimodal filler loadings from our experiments also exhibit lower values (Tables 2 and 3). These findings indicate that the application of close-packed structures in filler formulations is an idealized model that deviates significantly from reality, and that RLP is more likely to be the real packing arrangement.

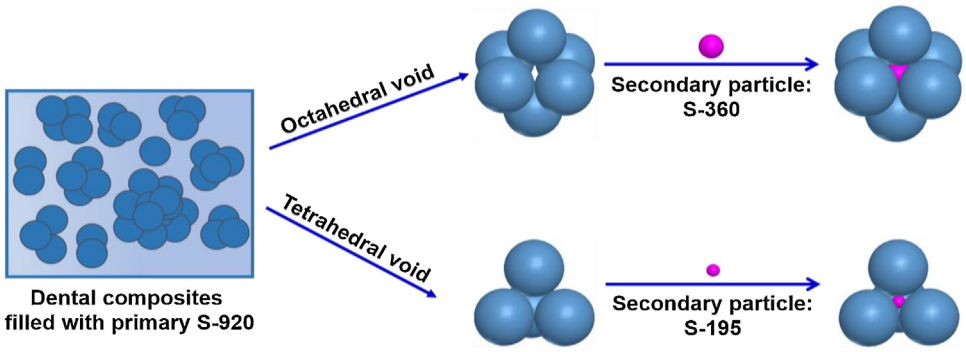

Fig. 2 – Representative illustration of the theoretical void models of the trimodal filler S-920+360+195, based on the close-packing of S-920.

The actual loading values of the bimodal and trimodal fillers further confirm this inference.

Considering the difference in the resin matrix, the 5B5T resin allows more secondary fillers to be incorporated in practice and has a higher filler loading than 7B3T for each filler formulation from theory to practice. The reason might just be due to the lower density of 5B5T ($\rho = 1.05\ g/cm^3$ vs $\rho = 1.11\ g/cm^3$ for 7B3T) in the calculations of the maximum loadings from theory to practice.

3.3. *Properties of experimental dental composites*

3.3.1. *Mechanical properties*

Mechanical tests were performed on the maximally loaded composites (Fig. 3). As expected, in comparison to S-920, there is an increasing trend in FS, FM, and CS with the addition of secondary particles for both 7B3T and 5B5T-based dental composites. Of all composite materials, the composite of 5B5T filled with S-920+360+195 exhibited the best mechanical performance. These results indicate that the higher filler loading obtained as a result of the optimized filler formulations imparts superior mechanical properties to the final materials, which is in agreement with previous reports [3,27].

3.3.2. *Degree of conversion*

Degree of conversion of dental composites is shown in Fig. 4A. With respect to S-920, the addition of secondary silica produces the final composites with increased conversion values for both resins, but the difference is not statistically significant. Raising the amount of Bis-GMA from 50 to 70 wt% in the resin matrix leads to a reduced conversion of all final composites, which agrees with previous reports [28–30]. Since Bis-GMA has a far higher viscosity than TEGDMA, a higher concentration of Bis-GMA in the 7B3T resin reduces the mobility of the system and hence the conversion.

3.3.3. *Depth of cure*

The depth of cure result shows similar results as the conversion of dental composites (Fig. 4B). The 5B5T resins have a higher depth of cure than 7B3T for each filler formulation. This is likely due to the refractive index (RI) difference between the resin and the filler particles. The light scattering, reflection, and refraction effects that lead to the opacity in these composites are governed by RI [31,32]. RI values of 7B3T and 5B5T are 1.52 and 1.507, respectively [33,34], such that the 5B5T resin matches more closely that of silica particles (1.46) [35], leading to the superior depth of cure. Moreover, for the 5B5T resin, only the addition of S-195 in the composite S-920 produced significant higher depth of cure, although the filler loading was increased slightly. This was expected due to the decreased light scattering and reflection by the smaller particles [3].

3.3.4. *Polymerization shrinkage*

Polymerization shrinkage of dental composites shows dependence on the filler formulations and the monomeric constitution. As shown in Fig. 5, the lowest shrinkage for 7B3T and 5B5T is obtained with S-920+360+195, which is decreased by 19 and 17%, respectively, in comparison to the values obtained using S-920 alone ($p < 0.05$). Such a phenomenon may be explained by the fact that both the higher filler loading of S-920+360+195 and the lower TEGDMA content in 7B3T decrease the overall density of C=C double bonds in the composites [18,36,37], therefore reducing the polymerization shrinkage to 2.13 ± 0.08%, the lowest value obtained in this study. The value represents a much-reduced shrinkage in comparison with the work by Miao et al. [38] who obtained the polymerization shrinkage of 2.69% using 7B3T as the resin and silica microspheres (diameter: 400 nm) as fillers in the dental composites (filler loading at 71 wt%). The reduction can be attributed to the higher loading of the mixed particles S-920+360+195 (72.08 wt%).

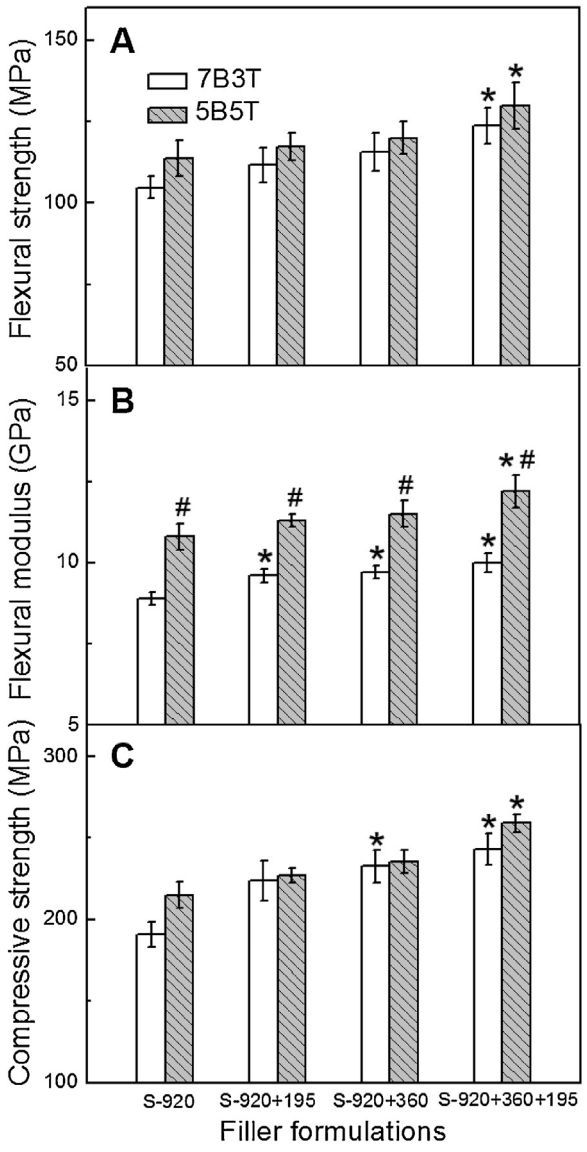

Fig. 3 – Flexural strength (A), flexural modulus (B), and compressive strength (C) of dental composites as a function of filler compositions for different Bis-GMA: TEGDMA mass ratios. *$p < 0.05$, compared with the S-920 filled composite with the same resin, and #$p < 0.05$, compared with the 7B3T-based composite at each filler formulation.

Table 3 – Theoretical and experimental maximum loading values of filler formulations, using 5B5T and 7B3T resins.

Filler formulation	Maximum filler loading							
	Theoretical estimation (wt%)						Experimental result (wt%/vol%)	
	FCC/HCP[a]		RCP[b]		RLP[c]			
	7B3T	5B5T	7B3T	5B5T	7B3T	5B5T	7B3T	5B5T
S-920	84.98	85.67	77.89	78.84	70.78	71.92	70.00/54.07	70.80/52.69
S-920+195	86.37	87.01	–	–	–	–	70.70/56.88	71.54/55.74
S-920+360	87.86	88.44	–	–	–	–	71.58/60.56	72.41/59.55
S-920+360+195	88.74	89.29	–	–	–	–	72.08/62.73	72.92/61.83

[a] Face centered cubic and hexagonal close packed.
[b] Random close packing.
[c] Random loose packing.

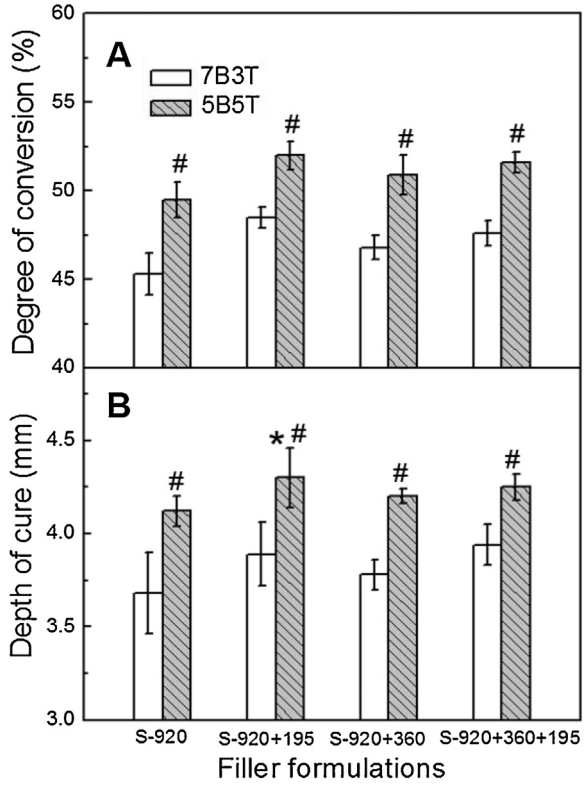

Fig. 4 – Degree of conversion (A), and depth of cure (B) of dental composites as a function of filler compositions for different Bis-GMA: TEGDMA mass ratios. *p < 0.05, compared with the S-920 filled composite with the same resin, and #p < 0.05, compared with the 7B3T-based composite at each filler formulation.

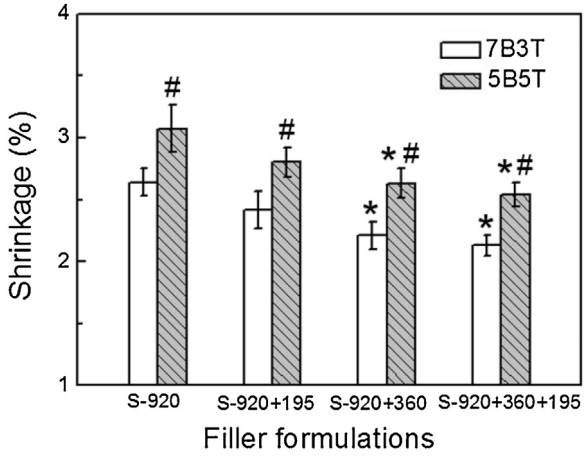

Fig. 5 – Polymerization shrinkage of dental composites as a function of filler compositions for different Bis-GMA: TEGDMA mass ratios. *p < 0.05, compared with the S-920 filled composite with the same resin, and #p < 0.05, compared with the 7B3T-based composite at each filler formulation.

3.3.5. *Surface morphology of fractured dental composites*

Representative fracture surfaces of 7B3T-based dental composites are selected so as to investigate the interaction between resin and fillers and the packing structures of fillers. As seen in Fig. 6(A–D), few exposed particles are observed in the composites, although the fillers are maximally loaded, indicating the good interfacial bonding of silica particles to the resin matrix [20]. Additionally, primary S-920 and secondary particles are randomly packed, confirming the close-packed structures cannot be achieved in practice.

3.3.6. *Viscosity properties*

The addition of inorganic fillers totally changes the flow of the uncured materials. As seen in Fig. 7, all dental composites show a strong non-Newtonian shear-thinning behavior, i.e., the complex viscosity decreases as the frequency increases, known as pseudoplasticity. For the two resin resins, as the content of secondary silica particles increased, the complex viscosity of trimodal silica fillers (S-920+360+195) reached a maximum value, which was followed by S-920+360, S-920+195, and S-920. These viscosity changes are due to the higher filler loading, in agreement with previous work [12]. Complex viscosity of the materials also has a strong dependence on the compositions of resin monomers. An exponential increase is observed for dental composites with more viscous 7B3T resin for each filler formulation in comparison with 5B5T [11]. Therefore, both filler formulations and resin monomers have an effect on composite viscosity.

In this work, we only use the two largest allowed sizes of spherical secondary particles that could fit into the tetrahedral and octahedral voids of the close-packed structures. It would be interesting to introduce commensurately smaller

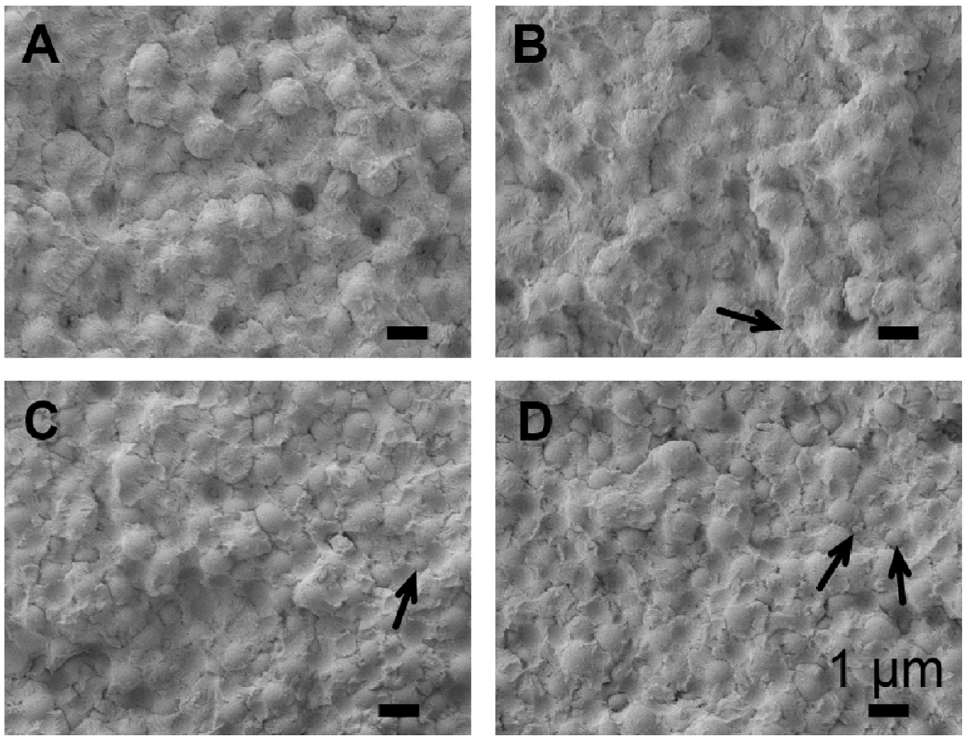

Fig. 6 – FE-SEM images of 7B3T-based dental composites filled with S-920 (A), S-920+195 (B), S-920+360 (C), and S-920+360+195 (D). Black arrows in (A–D) indicate the secondary silica particles in dental composites.

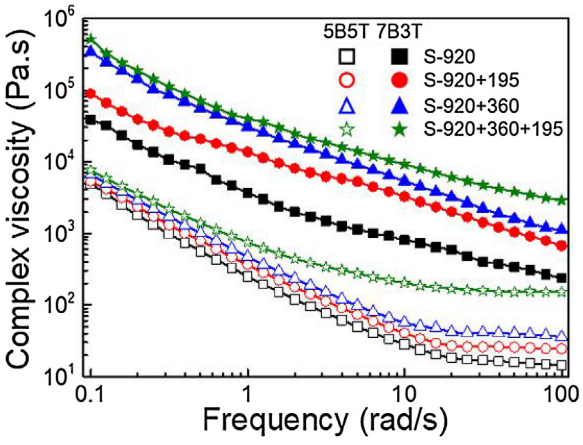

Fig. 7 – Complex viscosity of dental composites with different filler compositions and resin monomers as a function of shear frequency.

particles to fill the voids of the primary particles in the dental composites to obtain a more complete understanding of the effect of secondary filler size on the resin properties. Further studies on new preparation methods of dental composites and less viscous resin mixtures may lead to composites that may resemble more closely to the ideal packing of the particles in such composite materials. Additionally, the packing properties of irregular particles would also be interesting and useful to be conducted. All these will provide a better guidance in the optimization of dental formulations by the use multimodal fillers.

4. Conclusion

Two theoretical models, the close-packed structures and the random-packed structures of identical spherical particles, were examined in this work. The models based on close-packed structures of spherical particles may be idealized and over-simplified, but they still provide a convenient shortcut toward the optimal formulation of dental composites. The maximum allowed loadings of primary silica (S-920), and its filler mixtures with smaller secondary silica were investigated from theory to practice with two resin systems. First, the results and analyses presented herein indicate that random loose packing rather than the idealized close-packed structures more closely matches the real packing arrangement. Second, the addition of secondary particles into the maximally loaded S-920 composite further increased the total filler loading, especially the use of two different secondary particles of different sizes, leading to the improved mechanical properties, the reduced polymerization shrinkage, and the increased viscosity of the final composites. Third, despite the deviation of the reality from the idealized theory, the theoretical calculations may be used as guidance in the optimization of filler formulations and the properties of dental composites. As for the organic resin mixtures, the composites formulated with 5B5T produced stronger, higher conversion and higher depth of cure than 7B3T, due to the lower viscosity of 5B5T, but the composites with the more viscous 7B3T resin showed a lower polymerization shrinkage. It is rather hard to optimize all the properties of dental composites at the same time with one formulation, but the evaluation of the parameters that affect

the different properties of the dental composites can help to achieve the best overall performance of the material. In addition, the preparation methods (mixing technique, sequence of mixing, etc.) for the dental composites might be factors that affect the maximum filler loadings and the final properties. The three-roll mixer was used in this work and other mixing techniques may be evaluated.

Acknowledgments

This work was financially supported by NSERC and CIHR (grant number: CHRPJ 385852-10), National Key Research and Development Program of China (2016YFA0201702/2016YFA0201700), and Initial Research Funds for Young Teachers of Donghua University (grant number: 106-07-0053067).

Appendix A. Supplementary data

Supplementary data associated with this article can be found, in the online version, at https://doi.org/10.1016/j.dental.2018.03.022.

REFERENCES

[1] Stansbury JW, Lemon MT, Lu H, Ding XZ, Lin Y, Ge JH. Conversion-dependent shrinkage stress and strain in dental resins and composites. Dent Mater 2005;21:56–67.
[2] Habib E, Wang RL, Wang YZ, Zhu MF, Zhu XX. Inorganic fillers for dental resin composites: present and future. ACS Biomater Sci Eng 2016;2:1–11.
[3] Habib E, Wang RL, Zhu XX. Monodisperse silica-filled composite restoratives mechanical and light transmission properties. Dent Mater 2017;33:280–7.
[4] Satterthwaite JD, Vogel K, Watts DC. Effect of resin-composite filler particle size and shape on shrinkage-strain. Dent Mater 2009;25:1612–5.
[5] Satterthwaite JD, Maisuria A, Vogel K, Watts DC. Effect of resin-composite filler particle size and shape on shrinkage-stress. Dent Mater 2012;28:609–14.
[6] Turssia CP, Ferracanea JL, Vogel K. Filler features and their effects on wear and degree of conversion of particulate dental resin composites. Biomaterials 2005;26:4932–7.
[7] Wang RL, Habib E, Zhu XX. Application of close-packed structures in dental resin composites. Dent Mater 2017;33:288–93.
[8] Callister WD, Rethwisch DG. The structure of crystalline solids. In: Materials science and engineering: an introduction. New York: John Wiley & Sons, Inc; 2007. p. 38–79.
[9] Woodcock LV. Entropy difference between the face-centred cubic and hexagonal close-packed crystal structures. Nature 1997;385:141–3.
[10] Hong LH, Wang Y, Wang L, Zhang H, Na H, Zhang ZM. Synthesis and characterization of a novel resin monomer with low viscosity. Dent Mater 2017;59:11–7.
[11] Al-Ahdal K, Silikas N, Watts DC. Rheological properties of resin composites according to variations in composition and temperature. Dent Mater 2014;30:517–24.
[12] Lee JH, Um CM, Lee IB. Rheological properties of resin composites according to variations in monomer and filler composition. Dent Mater 2006;22:515–26.
[13] Beun S, Bailly C, Dabin A, Vreven J, Devaux J, Leloup G. Rheological properties of experimental Bis-GMA/TEGDMA flowable resin composites with various macrofiller/microfiller ratio. Dent Mater 2009;25:198–205.
[14] Stöber W, Fink A, Bohn E. Controlled growth of monodisperse silica spheres in the micron size range. J Colloid Interface Sci 1968;26:62–9.
[15] Wang RL, Habib E, Zhu XX. Synthesis of wrinkled mesoporous silica and its reinforcing effect for dental resin composites. Dent Mater 2017;33:1139–48.
[16] Wang XY, Cai Q, Zhang XH, Wei Y, Xu MM, Yang XP, Ma Q, Cheng YL, Deng XL. Improved performance of Bis-GMA/TEGDMA dental composites by net-like structures formed from SiO_2 nanofiber fillers. Mater Sci Eng C Mater Biol Appl 2016;59:464–70.
[17] Manojlovic D, Dramicanin MD, Lezaja M, Pongprueksa P, Van Meerbeek B, Miletic V. Effect of resin and photoinitiator on color, translucency and color stability of conventional and low-shrinkage model composites. Dent Mater 2016;32:183–91.
[18] Garoushi S, Vallittu PK, Watts DC, Lassila LV. Effect of nanofiller fractions and temperature on polymerization shrinkage on glass fiber reinforced filling material. Dent Mater 2008;24:606–10.
[19] Wang RL, Zhang ML, Liu FW, Bao S, Wu TT, Jiang XZ, et al. Investigation on the physical-mechanical properties of dental resin composites reinforced with novel bimodal silica nanostructures. Mater Sci Eng C Mater Biol Appl 2015;50:266–73.
[20] International Standard. Dentistry-polymer-based restorative materials. ISO-4049; 2009.
[21] Walters NJ, Xia W, Salih V, Ashley PF, Young AM. Poly(propylene glycol) and urethane dimethacrylates improve conversion of dental composites and reveal complexity of cytocompatibility testing. Dent Mater 2016;32:264–77.
[22] Beun S, Bailly C, Devaux J, Leloup G. Rheological properties of flowable resin composites and pit and fissure sealants. Dent Mater 2007;24:548–55.
[23] Gupta KM, Gupta N. Advanced electrical and electronics materials: processes and applications. In: Tiwari A, editor. Solid structures, characterization of materials, crystal imperfections, and mechanical properties of materials. Massachusetts and New Jersey: Scrivener Publishing LLC and John Wiley & Sons, Inc; 2015. p. 71–108.
[24] Onoda GY, Liniger EG. Random loose packings of uniform spheres and the dilatancy onset. Phys Rev Lett 1990;64:2727–30.
[25] Delaney GW, Hilton JE, Cleary PW. Defining random loose packing for nonspherical grains. Phys Rev E 2011;83:051305.
[26] Song CM, Wang P, Makse HA. A phase diagram for jammed matter. Nature 2008;453:629–32.
[27] Gonçalves F, Azevedo CLN, Ferracane JL, Braga RR. BisGMA/TEGDMA ratio and filler content effects on shrinkage stress. Dent Mater 2011;27:520–6.
[28] Dickens SH, Stansbury JW, Choi KM, Floyd CJE. Photopolymerization kinetics of methacrylate dental resins. Macromolecules 2003;36:6043–53.
[29] Dewaele M, Boutry DT, Devaux J, Leloup G. Volume contraction in photocured dental resins: the shrinkage-conversion relationship revisited. Dent Mater 2006;22:359–65.
[30] Lovell LG, Stansbury JW, Syrpes DC, Bowman CN. Effects of composition and reactivity on the reaction kinetics of dimethacrylate/dimethacrylate copolymerizations. Macromolecules 1999;32:3913–21.

[31] Schulz H, Burtscher P, Mädler L. Correlating filler transparency with inorganic/polymer composite transparency. Composites A: Appl Sci Manuf 2007;38:2451–9.
[32] Liu FW, Jiang XZ, Zhang QH, Zhu MF. Strong and bioactive dental resin composite containing poly(Bis-GMA) grafted hydroxyapatite whiskers and silica nanoparticles. Compos Sci Technol 2014;101:86–93.
[33] Howard B, Wilson ND, Newman SM, Pfeifer CS, Stansbury JW. Relationships between conversion, temperature and optical properties during composite photopolymerization. Acta Biomater 2010;6:2053–9.
[34] Khatri CA, Stansbury JW, Schultheisz CR, Antonucci JM. Synthesis, characterization and evaluation of urethane derivatives of Bis-GMA. Dent Mater 2003;19:584–8.
[35] García SF, Míguez H, Ibisate M, Meseguer F, López C. Refractive index properties of calcined silica submicrometer spheres. Langmuir 2002;18:1942–4.
[36] Gonçalves F, Kawano Y, Braga RR. Contraction stress related to composite inorganic content. Dent Mater 2010;26:704–9.
[37] Floyd CJ, Dickens SH. Network structure of Bis-GMA- and UDMA-based resin systems. Dent Mater 2006;22:1143–9.
[38] Miao XL, Li YG, Zhang QH, Zhu MF, Wang HZ. Low shrinkage light curable dental nanocomposites using SiO_2 microspheres as fillers. Mater Sci Eng C Mater Biol Appl 2012;32:2115–21.